Clim. Past Discuss., 8, 145–168, 2012
www.clim-past-discuss.net/8/145/2012/
doi:10.5194/cpd-8-145-2012

Climate
of the Past
Discussions

Interpreting last glacial to Holocene dust changes at Talos Dome (East Antarctica): implications for atmospheric variations from regional to hemispheric scales

S. Albani[1,2], B. Delmonte[1], V. Maggi[1], C. Baroni[3], J.-R. Petit[4], B. Stenni[5], C. Mazzola[1], and M. Frezzotti[6]

[1]Department of Environmental Sciences, University of Milano-Bicocca, Milano, Italy
[2]Graduate School in Polar Sciences, University of Siena, Siena, Italy
[3]Dipartimento di Scienze della Terra, Università di Pisa, Pisa, Italy
[4]LGGE-CNRS Université Joseph Fourier-Grenoble, Grenoble, France
[5]Dipartimento di Geoscienze, Università di Trieste, Trieste, Italy
[6]ENEA, Roma, Italy

Received: 20 December 2011 – Accepted: 23 December 2011 – Published: 5 January 2012

Correspondence to: S. Albani (samuel.albani@unimib.it)

Published by Copernicus Publications on behalf of the European Geosciences Union.

Abstract

Central East Antarctica ice cores preserve stratigraphic records of mineral dust originating from remote sources in the Southern Hemisphere, and represent useful indicators of climatic variations on glacial-interglacial time scales. The peripheries of the East Antarctic Ice Sheet, where ice-free areas with the potential to emit dust exist, have been less explored from this point of view. Here we present a new profile of dust deposition flux and grain size distributions from an ice core drilled at Talos Dome (Northern Victoria Land, East Antarctica), where there is a significant input of dust from proximal Antarctic ice-free areas. We analyze dust and stable water isotopes variations from the Last Glacial Maximum to the Late Holocene, and compare them to the EPICA Dome C profiles from Central East Antarctica. The smaller glacial-interglacial variations at Talos Dome compared to Dome C, and a distinctive decreasing trend during the Holocene, characterize the TALDICE dust profile. By deciphering the composite dust signal from both remote and local sources, we show the potential of this combined proxy of source activity and atmospheric transport to give information on both regional and larger spatial scales. In particular, we show how a regional signal, which we related to the deglaciation history of the Ross Sea embayment, can be superimposed to the broader scale glacial-interglacial variability that characterizes other Antarctic sites.

1 Introduction

Mineral dust is an active component of the climate system, interacting directly and indirectly with solar radiation, clouds and biogeochemistry (IPCC, 2007). It is emitted by the action of wind stress on arid or semiarid areas, with low vegetation cover and the capacity of accumulating fine-grained material (Prospero et al., 2002); as such, dust source areas may vary both in terms of activity and geographical location or size in response to environmental changes. Once entrained in the atmosphere, small dust grains can be transported over large distances by winds before they are deposited to the surface (Prospero et al., 2002). In environmental settings where formation and preservation of a continuous and undisturbed stratigraphy is likely, mineral dust represents a proxy for past climate, atmospheric and environmental changes (Kohfeld and Harrison, 2001).

Ice cores are considered invaluable climate archives (EPICA Community Members, 2004; Steffensen et al., 2008). Dust records from ice cores have been produced from both low-latitudes (Thompson et al., 1995; Xu et al., 2010) and polar ice caps (Petit et al., 1999; Lambert et al., 2008), preserving information on past variability of the dust cycle. In particular, dust records from polar ice cores have been shown to be very reliable indicators of climate variability on glacial-interglacial time scales (Fuhrer et al., 1999; Lambert et al., 2008). Most of the more detailed information on dust deposition in Antarctica on glacial-interglacial time scales stems from ice cores drilled in the Central East Antarctic Plateau (CEAP), e.g. Vostok (Petit et al., 1999) and EPICA Dome C (EDC) (Lambert et al., 2008). All sites from CEAP can be considered rather homogeneous in terms of snow accumulation rates, dust depositional fluxes, glacial-interglacial ratio of dust deposition and remote dust sources (Delmonte et al., 2004, 2008a). On the other hand, the peripheries of the East Antarctic ice sheet are still poorly explored from this point of view.

We present here a new mineral dust record spanning the period from 2 to 23 kyr Before Present (BP) obtained from the TALos Dome Ice CorE drilling project (TALDICE) ice core. Talos Dome (159°11′ E, 72°49′ S, 2315 m a.s.l., Fig. 1), is a peripheral dome located in the South Pacific/Ross Sea sector of the East Antarctic Plateau (see: www.taldice.org). The uppermost 1550 m of the 1620 m deep TALDICE ice core provide an undisturbed record of paleoclimate for the Ross Sea sector of East Antarctica covering the past 250 000 yr (Stenni et al., 2011). The geographic location of the drilling site, with relatively high snow accumulation rates (80 kg m^{-2} yr^{-1}, average 2004–1259 AD), enables accurate dating of the core, particularly during the last climatic transition (Buiron et al., 2011). The site also provided a good relative chronological link with other relevant Antarctic and Greenland ice cores (Lemieux-Dudon et al., 2010).

The climatic history of TALDICE was depicted by stable water isotopes (δ^{18}O) profiles, in comparison with other Antarctic sites. Some differences highlighted Talos Dome's more "coastal" behaviour compared to sites from CEAP, with distinctive features that could reflect changes in local elevation and/or in moisture source and pathways linked to the retreat of the Ross Ice Shelf and thinning of the peripheries of the East Antarctic Ice Sheet during the deglaciation (Stenni et al., 2011; Masson-Delmotte et al., 2011).

Previous work has shown that dust deposition at TALDICE responded to large climate variations on glacial-interglacial time scales, similar to the CEAP sites, with higher fluxes during cold stages (Delmonte et al., 2010b), when TALDICE and CEAP sites had a similar dust isotopic composition, suggesting common dust sources (Delmonte et al., 2010a). On the other hand, a different dust isotopic composition between TALDICE and CEAP sites during the Holocene, together with the presence of dust grains larger than 5 µm (diameter), that were virtually absent in the EDC core, highlight the significant contribution of dust of local origins to the TALDICE dust content (Delmonte et al., 2010b). The likely candidates to act as local dust sources are the widespread high-elevation ice-free areas of Northern Victoria Land (Delmonte et al., 2010b).

In this work, we present and analyze a higher resolution dust record, and in the light of previous works (Delmonte et al., 2010a,b), we carry out a closer inspection of dust flux and grain size variability with respect to the TALDICE stable water isotopes (δ^{18}O) profile, and compare this profile to EDC, which is assumed as representative of CEAP sites. In this comparative dust-δ^{18}O Talos Dome versus CEAP analysis throughout the deglaciation and the Holocene, we explore possible links between dust sources, atmospheric variations and the deglaciation history of the Ross Seas embayment.

2 Analytical methods

In this work, we present 549 discrete (25 cm long) ice sections in the 175–870 m depth range, corresponding to the ~2–23 kyr BP time period (Buiron et al., 2011), with an average time resolution of one sample every ~30 yr for the Holocene (average sample time span ~5 yr) and the deglaciation and one sample every ~350 yr for the LGM (average sample time span ~23 yr). Samples were decontaminated in a clean room (class 1000) under a laminar flow bench (class 100) following the procedure adopted in Delmonte et al. (2004, 2010b). Post-melt, samples were settled for 24 h and then analyzed for their insoluble mineral dust concentration and size. This was done to avoid the counting of metastable compounds that may be still in the solution immediately after melting (Sala et al., 2008). The analyses of dust concentration (number and volume) and size were performed at the University of Milano-Bicocca using a Beckman Coulter-Multisizer™ 3 Coulter Counter®, with three replicate measurements for each sample. The size range of the measurements was 1–30 µm. Mass concentration was calculated assuming a 2.5 $\mathrm{g\,cm^{-3}}$ of particle density (e.g. Petit et al., 1999). The dust concentration profile was then compared for inter-laboratory calibration with measurements from the LGGE in Grenoble (Delmonte et al., 2010b). A fine Particles Percentage (FPP) metric was used to describe dust size distributions, following Delmonte et al. (2004). The age profiles were based on the TALDICE-1 timescale (chronological uncertainties: ±300 yr from 8 to 15 kyr BP, ±500 yr back to 17.5 kyr and up to ±1500 yr during the Last Glacial Maximum – LGM) (Buiron et al., 2011). Dust depositional fluxes were calculated as dust concentration (mg dust per kg of ice/firn) multiplied by the ice/snow accumulation rate ($\mathrm{kg\,m^{-2}\,yr^{-1}}$) from Buiron et al. (2011).

3 The TALDICE dust profile: main features

Typical examples of dust measurements from the TALDICE ice core are shown in Fig. 2. Generally speaking, the mass (volume) size distributions of dust in the TALDICE samples (< 5 µm size range) are characterized by a poor size sorting during the current interglacial period (Fig. 2a), but shaped as lognormal distributions with a variable modal value around 2 µm during the LGM (Fig. 2b). In addition, particles in the 5–10 µm range are present in significant amount in our samples, in contrast with CEAP sites, where they are virtually absent (Delmonte et al., 2004). We compared our set of samples against a set of 150 blanks, in terms of number concentration, by applying a 1-tailed t-test ($\alpha = 0.05$). The results for the 1–5 µm and the 5–10 µm range indicate that 100 % and ~95 % of the samples were significantly higher than the blanks, with average signal-to-noise ratio of 40 and 15, respectively. We then calculated the measurements uncertainties, defined as the ratio between the standard deviation of the mean and the mean from the three replicates, and express them as percentages. The 90th percentile of uncertainties is 5 and 10 % for the 1–5 µm and the 5–10 µm range, respectively. These findings confirm the preliminary results from Delmonte et al. (2010b).

The main features of the TALDICE dust profile are shown in Fig. 3, together with the δ^{18}O profile (Fig. 3a), a proxy of local temperature at the Talos Dome site (Stenni et al., 2011). Both the dust mass concentration (Fig. 3b) and the depositional flux profiles (Fig. 3c) (1–5 µm size range) show large variability associated with glacial-interglacial changes, confirming the preliminary results from Delmonte et al. (2010b). Dust concentration measurements were compared with the set of samples analyzed in Grenoble (Delmonte et al., 2010b), which show a similar pattern and absolute values (Fig. 3b). Comparison of concentration and flux profile trends provides a mechanism to check whether changes in accumulation rates are the sole controlling factor (see the definition of flux in Sect. 2). Here, this is not the case (cfr. Fig. 3b,c). Flux, which represents the absolute deposition rate at the site, and allows for direct comparison with other sites, will be discussed instead of the concentration profile through the rest of the paper.

The 5–10 µm dust flux profile (Fig. 3d) resembles the finer fraction (1–5 µm) complementary profile, but the absolute values of the first are smaller and variations on the glacial-interglacial timescale look smoother. The 5–10 µm size fraction accounts for ~8 % of the total mass in the 1–10 µm range during the LGM, and ~21–25 % in the Holocene, on average.

Following Delmonte et al. (2004) we plotted the FPP metric (Fig. 3e), which shows a larger relative abundance of finer particles during the LGM compared to the Holocene. This pattern is qualitatively similar to that of EDC (Delmonte et al., 2004; Lambert et al., 2008), but a direct comparison is complicated by the presence of dust from local sources in TALDICE (Delmonte et al., 2010b). While for the 5–10 µm size fraction we may assume that all of the dust is from local sources (Delmonte et al., 2010b), it seems reasonable to consider dust in the 1–5 µm fraction as a mixture of particles from both local and remote sources, with unknown relative proportions, in principle. Complementary to FPP, we use the [1–5 µm]/[5–10 µm] size metric, which also shows a larger relative abundance of finer particles in the LGM-Holocene comparison (Fig. 3f).

4 Discussion

The starting point of our discussion is the contribution of dust from both remote and local sources to TALDICE. While the dust isotopic composition indicates Southern South America as the primary dust source during glacial periods for both EDC and TALDICE (Delmonte et al., 2010a), a possible contribution of Australia as a secondary but significant dust source to the Talos Dome area – more than for the CEAP – is suggested by climate models, although those do not account for Antarctic sources (Li et al., 2008; Albani et al., 2011). Given the predominant contribution of local dust to the geochemical fingerprint of TALDICE, it is not possible to directly test this hypothesis (Delmonte et al., 2010b), nor to assess if time-varying relative contributions from remote sources differentiate EDC and TALDICE dust deposition.

First, we will examine the TALDICE dust-δ^{18}O relationship and its time evolution, and through the comparison with EDC (and by extension the CEAP), assumed to represent the remote dust end-member, we will try to isolate the two superposed signals of remote and proximal dust deposition (Sect. 4.1). Second, we will explore the relationship between the variations in the remote and local dust inputs to Talos Dome and climate and atmospheric changes (Sect. 4.2).

4.1 Comparing TALDICE and Central East Antarctic Plateau

The TALDICE dust-δ^{18}O relationship and its time evolution was compared with the CEAP information, represented by EDC (Fig. 4). The TALDICE (Buiron et al., 2011) and EDC (Lemieux-Dudon et al., 2010) age models used here have rather small relative chronological uncertainties (Stenni et al., 2011).

After the LGM, during the first stage of the deglaciation, which started almost synchronously all over Antarctica at 18.2 ±0.7 kyr BP (Termination I) (Stenni et al., 2011) (Fig. 4a,c), the TALDICE dust flux (Fig. 4b) shows a drop in its absolute values with a decreasing trend at a rate of 2.2 $\mathrm{mg\,m^{-2}\,yr^{-1}}$ per kyr until the onset of the Antarctic Cold Reversal (ACR). Two events known as the Antarctic Isotope Maxima (AIM1: 14.7 ± 0.3 kyr BP and AIM0: 11.9 ± 0.1 kyr BP) (Stenni et al., 2011) bracket the ACR temperature reversal. After reaching a relative minimum at AIM1, which can be identified despite the high scatter of the data, the TALDICE dust flux (Fig. 4b) increases synchronously with the δ^{18}O decline during the ACR (Fig. 4a), but the timing of the declining dust trend from 13.4 ± 0.4 BP and the following minimum (13.0 ± 0.4 kyr BP) anticipate respectively the δ^{18}O ACR/AIM0 transition (12.7 ± 0.4) and AIM0 (11.9 ± 0.1 kyr BP) (Stenni et al., 2011). The early Holocene is characterized by large variability in the dust flux at Talos Dome, with a maximum deposition at ~9 kyr BP. Yet, no clear liner trend is evident (Fig. 4b), resembling the δ^{18}O pattern (Fig. 4a). The main feature of the record during mid-Holocene is a clear declining trend in dust flux from ~8 kyr BP, which persists during the late-Holocene, at least for the period spanned by our data (Fig. 4b). This feature appears to be in good timing with the δ^{18}O increasing trend (Fig. 4a).

We can directly compare the time evolution of the dust flux at Talos Dome with EDC (and the CEAP) (Fig. 4b), and examine this in conjunction with the temperature history of both sites, as depicted by the δ^{18}O profiles (Fig. 4a,c, respectively). Both sites show a decrease in dust deposition fluxes on the glacial-interglacial time scale, but the absolute values (Table 1) – and the amplitude of these variations – are different: the LGM to Holocene flux ratio is ~22 for EDC and in general for CEAP, but ~4 to ~10 for TALDICE when the Early and the Late Holocene are considered, respectively. This should not be surprising, considering the fact that local sources contribute dust to TALDICE, but not to EDC (Delmonte et al., 2010b). Thus, the temporal variability of the interplay between local and remote dust deposition at Talos Dome may explain the differences in magnitude and temporal patterns with respect to the EDC dust flux, which is derived exclusively from remote sources (Delmonte et al., 2008) and can be considered representative of remote dust deposition on glacial-interglacial time scales for a broad area (Lambert et al., 2008; Mahowald et al., 2010).

During the LGM, the dust flux is apparently lower at TALDICE compared to EDC. At this time, dust at the Talos Dome is thought to be derived mainly from remote areas (Delmonte et al., 2010a). This apparent difference in the magnitude of the deposition at the two sites, at a time when they are characterized by a common geochemical fingerprint (Delmonte et al., 2010a), may be explained either by (1) a bias in TALDICE data related to the limited number of samples analyzed so far for the glacial period, compared to the large variability of the data during LGM, and/or (2) a relative dating error between the two sites for this time interval, influencing accumulation rates and dust fluxes, and/or (3) a real difference in dust flux from remote areas related to geographic position and atmospheric circulation. We will not discuss this further as this does not affect our interpretations and is beyond the scopes of this paper.

In correspondence of Termination I (18.2 ± 0.7 kyr BP) both TALDICE and EDC records show a decreasing trend, with similar dust fluxes both in terms of magnitude and rate of decrease (Fig. 4b), at the time of the drop in dust advection from remote sources (Lambert et al., 2008). After ~16 kyr BP the dust flux magnitudes and patterns clearly diverge, whereas the δ^{18}O patterns at TALDICE and EDC coherently evolve until ~12.5–12.7 kyr BP (the different absolute values of δ^{18}O reflect the different temperatures at the two sites) (Stenni et al., 2011). An apparent re-alignment of dust flux patterns occurs in correspondence of the onset of the ACR (Fig. 4b). The δ^{18}O profiles show a similar timing with the onset and termination of the ACR at TALDICE and EDC (Fig. 4a,c). While the EDC dust flux follows the same pattern, dust deposition at Talos Dome has original features: after ~13.5–13.7 kyr BP the two profiles are definitively different, with an early relative dust minimum at TALDICE around 13 kyr BP, which is absent in Central Antarctica. In addition, there is no evidence for the so-called "pre-Holocene dust minimum" (11.3–12.1 kyr BP) which has been found in different ice cores from Central Antarctica, and that was used for stratigraphic correlations (Delmonte et al., 2004). The TALDICE dust flux is highly variable beyond 13 kyr BP with a maximum around ~9 kyr BP, which is preceded by a marked and continuous decline from ~8 kyr BP (Fig. 4b). This inversely correlates with the δ^{18}O pattern, which is characterized by a rather stable profile during the early Holocene, preceding a relative minimum ~8 kyr BP followed by an increasing trend (Fig. 4a). At EDC, on the other hand, while the dust flux shows a quick recovery after the pre-Holocene dust minimum and then is characterized by a slight long-term Holocene decreasing trend (Delmonte et al., 2005) (Table 1), it does not seem to mimic the oscillations shown by the δ^{18}O pattern. The EDC pattern is characterized by an evident early Holocene "optimum" with low values, followed by a relative minimum and then by a slightly decline through the mid-Holocene (Fig. 4c).

During cold periods, when dust input from remote sources is large and a climate coupling between the mid-to-high southern latitudes exists (Petit et al., 1999; Lambert et al., 2008; Albani et al., 2011), e.g. the end of the LGM and ACR, the patterns of dust deposition between TALDICE and EDC are more similar than for periods characterized by lower remote dust input, such as the end of deglaciation and the Holocene. In addition, while the dust- δ^{18}O relation at EDC seems to be closer on the glacial-interglacial time scale than within the Holocene, at TALDICE the Holocene similarity in dust and δ^{18}O patterns is quite clear.

4.2 Linking TALDICE dust profile with climate and atmospheric changes

Understanding the factors controlling the variability of dust advection from local sources to Talos Dome is necessary in order to explain the whole TALDICE dust signal, as is the extent to which the regional atmospheric circulation modulates the variability of dust advection to Talos Dome. Work on water stable isotopes has shown how, when superimposed on variations in climate change patterns, differences in δ^{18}O profiles among Antarctic ice cores can be understood if site-specific properties are considered (Stenni et al., 2011; Masson-Delmotte et al., 2011). During the Holocene, the dust and δ^{18}O profiles at EDC do not vary proportionally, which is likely to be an expression of the remote nature of dust reaching the site, and indicative of changed conditions at the source areas and/or in the mid-to-high latitudes atmospheric connection (Lambert et al., 2008). The closer dust-δ^{18}O evolution at Talos Dome highlights the influence that local/regional changes had on the proximal dust contribution to the site. The main source of the differences between EDC and TALDICE δ^{18}O profile can be related to the retreat of the Ross Ice Sheet (the grounded Ross Ice Shelf during the glacial period) (Stenni et al., 2011). We explore the possible drivers of variability in local dust sources and transport to the Talos Dome site.

Potential proximal sources of dust for TALDICE include regoliths and Pleistocene glacial drifts located at high altitude in the Victoria Land. While some of these sources are known to have been active well beyond the Holocene and the LGM, some glacial sediments such as younger drifts became available during the last climatic cycle, and retreat moraines locally deposited during the deglaciation could have contributed dust after glacial maxima (Delmonte et al., 2010b and references therein). In the Talos Dome regional setting, the deglaciation initiated about 14 kyr BP at the Ross Ice Sheet margin, became widespread about 12 kyr BP, and was completed by about 8 kyr BP at Terra Nova Bay (Baroni and Hall, 2004; Baroni et al., 2005; Mackintosh et al., 2011).

Dust transported from remote sources long range generally reaches Antarctica through medium/high tropospheric pathways (Li et al., 2008; Krinner et al., 2010; Albani et al., 2011), although transport mechanisms acting in a competitive way may be responsible for differences in coastal areas compared to high-elevation inland sites (Delmonte et al., 2004; Krinner et al., 2010). On the other hand, because Talos Dome is located inland with respect to the ice-free source areas (Fig. 1), advection of air masses inland from the ocean is a necessary condition for the transport of local dust to the site. Presently, the Ross Sea sector around Terra Nova Bay is one of the most active areas of mesoscale cyclogenesis along the Antarctic coasts, particularly in the form of dry cyclogenesis, which near the Transantarctic Mountains can set up conditions for the development of barrier winds (Carrasco et al., 2003). Some sectors of the East Antarctic ice sheet facing the Southern Ocean receive moisture-laden air masses leading to snowfall mainly during the winter from western pathways, while Victoria Land is highly affected by the peculiar conditions in the Ross Sea, with additional eastern pathways during summer moving inland from the Ross Sea (Scarchilli et al., 2011). We can thus consider the TALDICE δ^{18}O profile, intrinsically related to precipitation events (Stenni et al., 2011), as a proxy of atmospheric pathways favourable for dust transport to Talos Dome from local sources.

While comparing the TALDICE and EDC dust flux in the 1–5 µm size range (Fig. 4b) provides an appreciation of the additional contribution of local sources at Talos Dome, it is easier to evaluate the variability of local dust if we also consider the 5–10 µm size range (Fig. 3d), which we assume as derived entirely from proximal sources. Dust flux in both size ranges shows variations in correspondence of Termination I and the ACR. Yet, the very limited changes of dust flux in the 5–10 µm fraction (Fig. 3d) suggests that advection from Antarctic sources varied only slightly in relation to the major climate changes. This is not the case for particles flux in the 1–5 µm range (Fig. 3c), which includes a contribution from both remote and proximal sources. It is interesting to note that the relative dust minimum in TALDICE dust flux at ~13 kyr BP, pre-dating the termination of the ACR, is evident in both size fractions (Fig. 3c,d). After this minimum, the dust flux in both size fractions increases again and shows large variability around relatively high values until 8–9 kyr BP, when it starts to decline. The higher absolute values of the 5–10 µm fraction flux in the early Holocene compared to the relative minima at AIM1 and 13 kyr BP suggest that the variable dust flux pattern between 13 and 9 kyr BP could be related to the initial retreat of the Ross Ice Sheet (Fig. 1) in response to the deglaciation (Mackintosh et al., 2011) – and associated formation of retreat moraine deposits that could act as new dust sources, in addition to those already active during the glacial period. Similarly, we can explain the pronounced Holocene decreasing dust trend starting around 8 kyr BP, observed in both size fractions (Fig. 3c,d), by considering two hypotheses: (1) the presence of local dust sources that underwent exhaustion during the Holocene or (2) changes in the atmospheric dust transport.

Based upon the hypothesis of an exhausting or reduced local source (formation of desert pavement on retreat moraine), a synchronous change in the dust grain size distribution, with an increasing 1–5 µm/5–10 µm ratio would be expected as a consequence of the weakening of the local source(s). This is not supported by the data, as the 1–5 µm/5–10 µm ratio (Fig. 3f) is variable but rather constant after the deglaciation.

If we invoke changes in transport of dust from local sources to Talos Dome to explain the Holocene decreasing trend in dust deposition, we should consider either (1) reduced frequency and/or intensity of maritime air mass advection related to the long-term increase of katabatic winds, or (2) a long-term shift of the preferred trajectories of air masses, on a climatological timescale, so that they invest to a lesser extent the potential source areas. Both hypotheses do not contradict with the constraints posed by the observed dust size distributions, and they are not mutually exclusive. Nonetheless, there are evidences pointing to a possible change in atmospheric pathways during the middle and late Holocene.

During the last glacial period, the presence of the Ross Ice Sheet affected the atmospheric circulation at a regional level: air masses trajectories, such as those that today bring moisture to the Talos Dome site through the Ross Sea, would have been largely hampered (Stenni et al., 2011). After the deglaciation, when most of the regional ice loss happened with the melting of the Ross Ice Sheet (Mackintosh et al., 2011), the opening of the Ross Sea embayment ~8 kyr BP marked the beginning of new phase of retreat of the Ross Ice Shelf (Conway et al., 1999). The process continued (Baroni and Orombelli, 1991; Baroni and Hall, 2004), albeit with temporal and spatial variability (Hall et al., 2006), throughout the Holocene before a neo-glacial re-advance during the last millennium (Hall, 2009). These events can indeed cause a consequent modification of the regional atmospheric circulation patterns, and are coeval with the decreasing trend in dust flux at Talos Dome, evident in both the 1–5 µm and the 5–10 µm size fractions. The TALDICE δ^{18}O profile (Fig. 4a) records such variations: the weaker amplitude of AIM0 compared with other East Antarctic Plateau sites (e.g. Fig. 4a) indicates longer and cooler distillation pathways, which could occur by transit over the Ross Sea after the Ross Ice Sheet retreat (Stenni et al., 2011). In addition, the TALDICE δ^{18}O profile (Fig. 3a) actually shows an increasing trend during the Holocene starting from ~8 kyr BP (Stenni et al., 2011; Masson-Delmotte et al., 2011), a signal that would be coherent with the progressively reduced ice cover in the Ross Sea embayment related to the retreat of the Ross Ice Shelf (Hall, 2009).

In this scenario, the non-glaciated areas located at high altitude in Northern Victoria Land, acting as sources for insoluble mineral dust, would be progressively less subject to Aeolian dust deflation by air masses coming from the North, with consequent reduced dust drift to Talos Dome. If the assumption that the mechanism depicted above is substantially correct, it seems reasonable to find a relationship between the deglaciation history in the Ross Sea Embayment and the decreasing trend of the TALDICE dust record during the Holocene.

5 Conclusions

The new dust record from the TALDICE ice core reflects both large-scale dust changes on glacial/interglacial time scales and a regional signal emerging when dust advection from remote sources was extremely low. Dust deposition at Talos Dome reflects the major climate changes occurring on a hemispheric scale during the last climatic transition, as suggested by the first-order variability of dust in the 1–5 µm size range between 2 and 23 kyr BP. However, the contribution from local dust sources makes Talos Dome sensitive to the regional atmospheric circulation changes in particular during warm climate periods, such as the end of Termination I and the Holocene.

The relatively high and variable dust deposition at Talos Dome during the last stages of the deglaciation and the early Holocene may reflect the enhanced availability of dust originated from proximal sources, i.e. from glacial drift left behind retreating glaciers during the initial phase of retreat of the Ross Ice Sheet between 13 and 9 kyr BP. Afterwards, we suggest that the decreasing trend in dust deposition from 8 kyr BP may be related to less favourable atmospheric transport from proximal dust sources, linked to the changes in atmospheric circulation in response to the progressive opening of the Ross Sea embayment. Thus, we found a possible link between the deglaciation history of the Ross Sea and the mesoscale atmospheric circulation, which modulates the local dust flux at Talos Dome. Future extension of the TALDICE dust record to the last millennium will allow verification of the response of dust to the neo-glacial re-advance in the Ross Sea (Hall, 2009). In addition, future comparisons with other proxies such as marine aerosols would help to further understand the atmospheric variability at the site.

Acknowledgements. The Talos Dome Ice core Project (TALDICE), a joint European programme, is funded by national contributions from Italy, France, Germany, Switzerland and the UK. Main logistic support was provided by PNRA. This is TALDICE publication no. ##. This work is a contribution to the PRIN 2009 research project "Variability and geographic provenance of eolian dust in Antarctica during the late Quaternary: a multi-parametric approach with the use of cutting-edge techniques". The HOLOCLIP Project, a joint research project of ESF Polar-CLIMATE programme, is funded by national contributions from Italy, France, Germany, Spain, Netherlands, Belgium and the United Kingdom. In Italy HOLOCLIP is funded by PNRA. This is HOLOCLIP publication no. ##. We also thank Yvette Wharton (University of Auckland) for her valuable comments to the English text. S. Albani acknowledges funding from "Dote Ricercatori": FSE, Regione Lombardia and the University of Milano-Bicocca for co-funding.

Title Page
Abstract Introduction
Conclusions References
Tables Figures
|◀ ▶|
◀ ▶
Back Close
Full Screen / Esc
Printer-friendly Version
Interactive Discussion

References

Albani, S., Mahowald, N. M., Delmonte, B., Maggi, V., and Winckler, G.: Comparing modeled and observed changes in mineral dust transport and deposition to Antarctica between the Last Glacial Maximum and current climates, Clim. Dynam., in press, doi:10.1007/s00382-011-1139-5, 2011.

Baroni, C. and Orombelli, G.: Holocene raised beaches at Terra Nova Bay, Victoria Land, Antarctica, Quaternary Res., 36, 157–177, 1991.

Baroni, C. and Hall, B. L.: A new Holocene relative sea-level curve for Terra Nova Bay, Victoria Land, Antarctica, J. Quaternary Sci., 19, 377–396, 2004.

Baroni, C., Frezzotti, M., Salvatore, M. C., Meneghel, M., Tabacco, I. E., Vittuari, L., Bondesan, A., Biasini, A., Cimbelli, A., and Orombelli, G.: Antarctic geomorphological and glaciological 1:250 000 map series, Mt. Murchison Quadrangle (Northern Victoria Land), explanatory notes (with geomorphological map at the scale of 1:250 000), Ann. Glaciol., 39, 256–264, 2005.

Buiron, D., Chappellaz, J., Stenni, B., Frezzotti, M., Baumgartner, M., Capron, E., Landais, A., Lemieux-Dudon, B., Masson-Delmotte, V., Montagnat, M., Parrenin, F., and Schilt, A.: TALDICE-1 age scale of the Talos Dome deep ice core, East Antarctica, Clim. Past, 7, 1–16, doi:10.5194/cp-7-1-2011, 2011.

Carrasco, J. F., Bromwich, D. H., and Monaghan, A. J.: Distribution and characteristics of mesoscale cyclones in the Antarctic: Ross Seas eastward to the Weddell Sea, Mon. Weather Rev., 131, 289–301, 2003.

Conway, H., Hall, B. L., Denton, G. H., Gades, A. M., and Waddington, E. D.: Past and future grounding-line retreat of the Western Antarctic ice sheet, Science, 286, 280–283, 1999.

Delmonte, B., Petit, J.-R., Andersen, K. K., Basile-Doelsch, I., Maggi, V., and Ya Lipenkov, V.: Dust size evidence for opposite regional atmospheric circulation changes over East Antarctica during the last climatic transition, Clim. Dynam., 23, 427–438, 2004.

Delmonte, B., Petit, J.-R., Krinner, G., Maggi, V., Jouzel, J., and Udisti, R.: Ice core evidence for secular variability and 200-year dipolar oscillations in atmospheric circulation over East Antarctica during the Holocene, Clim. Dynam., 24, 641–654, 2005.

Delmonte, B., Andersson, P. S., Hansson, M., Schöberg, H., Petit, J.-R., Basile-Doelsch, I., and Maggi, V.: Aeolian dust in East Antarctica (EPICA-Dome C and Vostok): provenance during glacial ages over the last 800 kyr, Geophys. Res. Lett., 35, L07703, doi:10.1029/2008GL033382, 2008.

Delmonte, B., Andersson, P. S., Schöberg, H., Hansson, M., Petit, J.-R., Delmas, R., Gaiero, D. M., Maggi, V., and Frezzotti, M.: Geographic provenance of aeolian dust in East Antarctica during Pleistocene glaciations: preliminary results from Talos Dome and comparison with East Antarctic and new Andean ice core data, Quaternary Sci. Rev., 29, 256–264, 2010a.

Delmonte, B., Baroni, C., Andersson, P. S., Schöberg, H., Hansson, M., Aciego, S., Petit, J.-R., Albani, S., Mazzola, C., Maggi, V., and Frezzotti, M.: Aeolian dust in the Talos Dome ice core (East Antarctica, Pacific/Ross Sea sector): Victoria Land versus remote sources over the last two climate cycles, J. Quaternary Sci., 25, 1327–1337, 2010b.

EPICA Community Members: Eight glacial cycles from an Antarctic ice core, Nature, 429, 623–628, 2004.

Fuhrer, K., Wolff, E. W., and Johnsen, S. J.: Timescales for dust variability in the Greenland Ice Core Project (GRIP) ice core in the last 100 000 years, J. Geophys. Res., 104, 31043–31052, 1999.

Hall, B. L.: Holocene glacial history of Antarctica and the sub-Antarctic islands, Quaternary Sci. Rev., 28, 2213–2230, 2009.

Hall, B. L., Hoelzel, A. R., Baroni, C., Denton, G. H., Le Boeuf, B. J., Overturf, J., and Töpf, A. L.: Holocene elephant seal distribution implies warmer-than-present climate in the Ross Sea, P. Natl. Acad. Sci. USA, 103, 10213–10217, 2006.

IPCC: Climate Change 2007: The Physical Science Basis. Contribution of Working Group I to the Fourth Assessment Report of the Intergovernmental Panel on Climate Change, edited by: Solomon, S., Qin, D., Manning, M., Chen, Z., Marquis, M., Averyt, K. B., Tignor, M., and Miller, H. L., Cambridge University Press, Cambridge, UK and New York, NY, USA, 996 pp., 2007.

Kohfeld, K. E. and Harrison, S. P.: DIRTMAP: the geological record of dust, Earth-Sci. Rev., 54, 81–114, 2001.

Krinner, G., Petit, J.-R., and Delmonte, B.: Altitude of atmospheric tracer transport towards Antarctica in present and glacial climate, Quaternary Sci. Rev., 29, 274–284, 2010.

Lambert, F., Delmonte, B., Petit, J.-R., Bigler, M., Kaufmann, P. R., Hutterli, M. A., Stocker, T. F., Ruth, U., Steffensen, J. P., and Maggi, V.: Dust-climate couplings over the past 800 000 years from the EPICA Dome C ice core, Nature, 452, 616–619, 2008.

Lemieux-Dudon, B., Blayo, E., Petit, J.-R., Waelbroeck, C., Svensson, A., Ritz, C., Barnola, J. M., Narcisi, B. M., and Parrenin, F.: Consistent dating for Antarctic and Greenland ice cores, Quaternary Sci. Rev., 29, 8–20, 2010.

Li, F., Ginoux, P., and Ramaswamy, V.: Distribution, transport, and deposition of mineral dust in the Southern Ocean and Antarctica: Contribution of major sources, J. Geophys. Res., 113, D10207, doi:10.1029/2007JD009190, 2008.

Mackintosh, A., Golledge, N., Domack, E., Dunbar, R., Leventer, A., White, D., Pollard, D., DeConto, R., Fink, D., Zwartz, D., Gore, D., and Lavoie, C.: Retreat of the East Antarctic ice sheet during the last glacial termination, Nat. Geosci., 4, 195–202, 2011.

Mahowald, N. M., Albani, S., Engelstaedter, S., Winckler, G., and Goman, M.: Model insight into glacial-interglacial paleodust records, Quaternary Sci. Rev., 30, 832–854, 2010.

Masson-Delmotte, V., Buiron, D., Ekaykin, A., Frezzotti, M., Gallée, H., Jouzel, J., Krinner, G., Landais, A., Motoyama, H., Oerter, H., Pol, K., Pollard, D., Ritz, C., Schlosser, E., Sime, L. C., Sodemann, H., Stenni, B., Uemura, R., and Vimeux, F.: A comparison of the present and last interglacial periods in six Antarctic ice cores, Clim. Past, 7, 397–423, doi:10.5194/cp-7-397-2011, 2011.

Petit, J.-R., Jouzel, J., Raynaud, D., Barkov, N. I., Barnola, J. M., Basile, I., Bender, M., Chappellaz, J., Davisk, M., Delaygue, G., Delmotte, M., Kotlyakov, V. M., Legrand, M., Lipenkov, V. Y., Lorius, C., Pepin, L., Ritz, C., Saltzman, E., and Stievenard, M.: Climate and atmospheric history of the past 420 000 years from the Vostok ice core, Antarctica, Nature, 399, 429–436, 1999.

Prospero, J. M., Ginoux, P., Torres, O., Nicholson, S. E., and Gill, T. E.: Environmental characterization of global sources of atmospheric soil dust identified with the Nimbus 7 Total Ozone mapping spectrometer (TOMS) absorbing aerosol product, Rev. Geophys., 40, 1002, doi:10.1029/2000RG000095, 2002.

Sala, M., Delmonte, B., Frezzotti, M., Proposito, M., Scarchilli, C., Maggi, V., Artioli, G., Dapiaggi, M., Marino, F., Ricci, P. C., and De Giudici, G.: Evidence of calcium carbonates in coastal (Talos Dome and Ross Sea area) East Antarctica snow and firn: environmental and climatic implications, Earth Planet. Sc. Lett., 271, 43–52, 2008.

Scarchilli, C., Frezzotti, M., and Ruti, P. M.: Snow precipitation at four ice core sites in East Antartica: provenance, seasonality and blocking factors, Clim. Dynam., 37, 2107–2125, 2011.

Steffensen, J. P., Andersen, K. K., Bigler, M., Clausen, H. B., Dahl-Jensen, D., Fischer, H., Goto-Azuma, K., Hansson, M., Johnsen, S. J., Jouzel, J., Masson-Delmotte, V., Popp, T., Rasmussen, S. O., Röthlisberger, R., Ruth, U., Stauffer, B., Siggaard-Andersen, M. L., Sveinbjörnsdóttir, A. E., Svensson, A., and White, J. W. C.: High-resolution Greenland ice core data show abrupt climate change happens in few years, Science, 321, 680-684, 2008.

Stenni, B., Masson-Delmotte, V., Selmo, E., Oerter, H., Meyer, H., Röthlisberger, R., Jouzel, J., Cattani, O., Falourd, S., Fischer, H., Hoffmann, G., Iacumin, P., Johnsen, S. J., Minster, B., and Udisti, R.: The deuterium excess records of EPICA Dome C and Dronning Maud Land ice cores (East Antarctica), Quaternary Sci. Rev., 29, 146–159, 2010.

Stenni, B., Buiron, D., Frezzotti, M., Albani, S., Barbante, C., Bard, E., Barnola, J. M., Baroni, M., Baumgartner, M., Bonazza, M., Capron, E., Castellano, E., Chappellaz, J., Delmonte, B., Falourd, S., Genoni, L., Iacumin, P., Jouzel, J., Kipfstuhl, S., Landais, A., Lemieux-Dudon, B., Maggi, V., Masson-Delmotte, V., Mazzola, C., Minster, B., Montagnat, M., Mulvaney, R., Narcisi, B., Oerter, H., Parrenin, F., Petit, J. R., Ritz, C., Scarchilli, C., Schilt, A., Schüpbach, S., Schwander, J., Selmo, E., Severi, M., Stocker, T. F., and Udisti, R.: Expression of the bipolar see-saw in Antarctic climate records during the last deglaciation, Nat. Geosci., 4, 46-49, doi:10.1038/ngeo1026, 2011.

Thompson, L. G., Mosley-Thompson, E., Davis, M. E., Lin, P. N., Henderson, K. A., Cole-Dai, J., Bolzan, J. F., and Liu, K. B.: Late-glacial stage and Holocene tropical ice core records from Huascarán, Peru, Science, 269, 46–50, 1995.

Xu, J., Hou, S., Qin, D., Kaspari, S., Mayewski, P. A., Petit, J.-R., Delmonte, B., Kang, S., Ren, J., Chappellaz, J., and Hong, S.: A 108.83-m ice-core record of atmospheric dust deposition at Mt. Qomolangma (Everest), Central Himalaya, Quaternary Res., 73, 33–38, 2010.

Table 1. Average dust deposition flux ($\text{mg}\,\text{m}^{-2}\,\text{yr}^{-1}$) for TALDICE (this work) and EDC (Delmonte et al., 2004) in three different sub-periods of the temporal window analysed in the text.

Period	TALDICE flux (1–5 µm)	EDC flux
Late Holocene (2–5 kyr BP)	0.70	0.33
Early Holocene (8–11.7 kyr BP)	1.84	0.47
LGM (18–23 kyr BP)	7.24	9.49

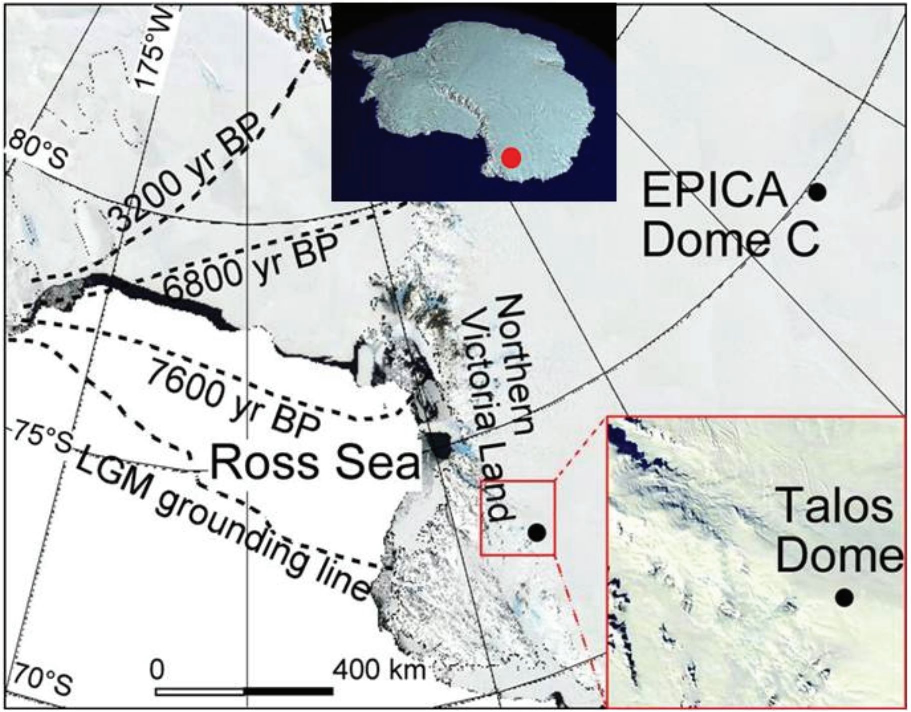

Fig. 1. Satellite image (Landsat Image Mosaic of Antarctica Project) of the Ross Sea and Dome C area. The top insert shows the approximate location of Talos Dome (red dot) in Antarctica (A RADARSAT Map of Antarctica. Credit: AMM, SVS, NASA, CSA. Source: http://apod.nasa.gov/apod/ap991116.html). The insert on the bottom-right side shows the Talos Dome area. Dashed lines with accompanying time indication show the timing of the Ross Ice Shelf grounding line retreat (Conway et al., 1999; Hall, 2009).

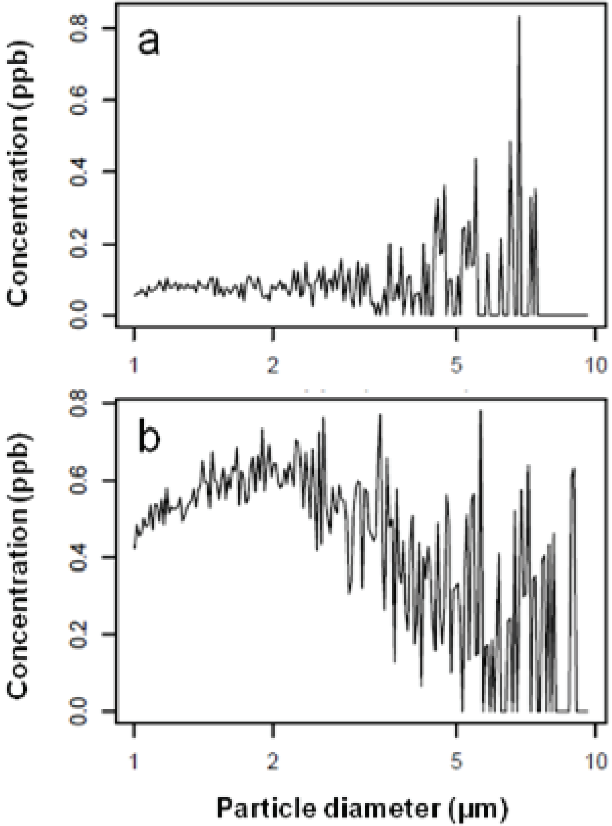

Fig. 2. Examples of dust size distributions from TALDICE ice core samples. **(a)** Late Holocene sample at 210.25 m depth. **(b)** Glacial sample at 802.00 m depth.

Title Page
Abstract
Introduction
Conclusions
References
Tables
Figures
◀▮
▶▮
◀
▶
Back
Close
Full Screen / Esc
Printer-friendly Version
Interactive Discussion

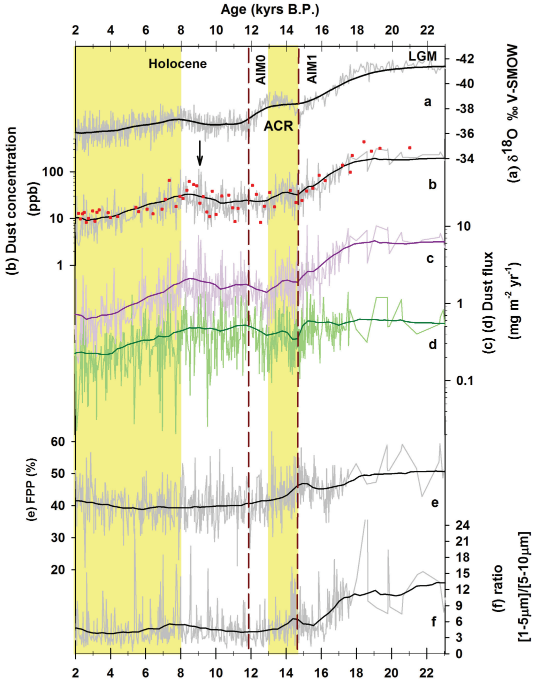

Fig. 3. TALDICE records of: **(a)** δ^{18}O ‰ V-SMOW (Stenni et al., 2011) plotted on a reversed axis; **(b)** dust concentration (ppb) in the [1–5] µm size range (grey line: Milano; red dots: Grenoble (Delmonte et al., 2010b)); **(c)** dust flux (mg m^{-2} yr^{-1}) in the [1–5] µm size range (purple line); **(d)** dust flux (mg m^{-2} yr^{-1}) in the [5–10] µm size range (green line); **(e)** FPP (%), defined as the [1–2]/[1–5] µm ratio (Delmonte et al., 2004); **(f)** ratio between the mass (volume) of particles in the 1–5 µm and 5–10 µm size intervals. Thin lines represent original data, superimposed thick lines mark the smoothed profiles (negative exponential with sampling proportion 0.1). The vertical dashed lines mark the AIM0 and AIM1 events. The arrow in **(b)** marks the Holocene dust maximum. Background yellow bands highlight features of the dust record described in the text: the Holocene decreasing trend (left) and the ACR (right).

Title Page
Abstract
Introduction
Conclusions
References
Tables
Figures
◀◀
▶▶
◀
▶
Back
Close
Full Screen / Esc
Printer-friendly Version
Interactive Discussion

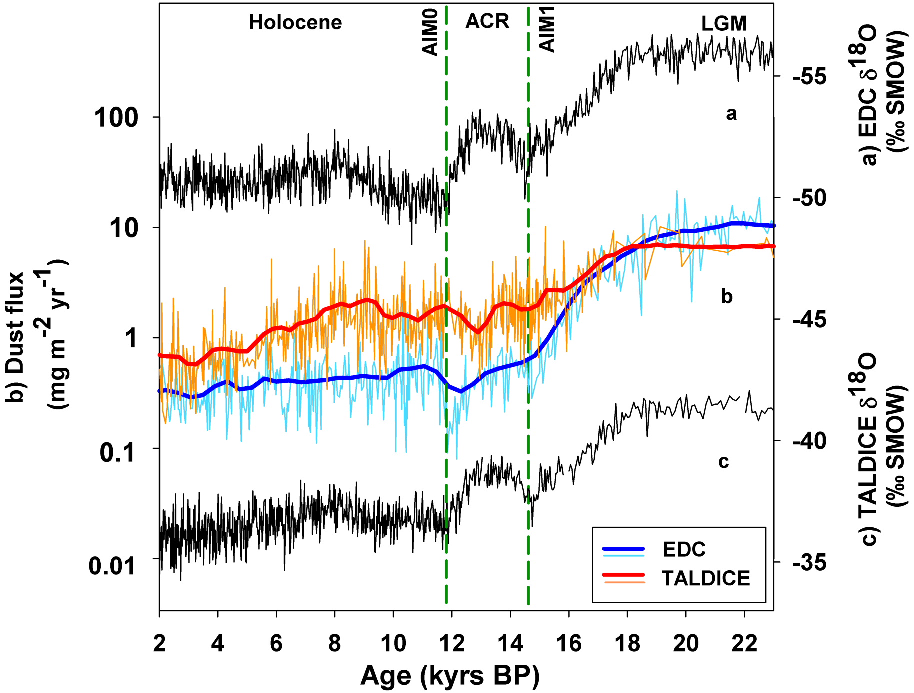

Fig. 4. Comparison of TALDICE and EDC dust fluxes (1–5 µm) and δ^{18}O profiles. **(a)** TALDICE δ^{18}O ‰ V-SMOW (Stenni et al., 2011) plotted on a reversed axis. **(b)** Age profiles of EDC flux (light blue line) and TALDICE flux (orange line). Superimposed thick lines are the smoothed profiles of EDC (dark blue) and TALDICE (red), respectively. **(c)** EDC δ^{18}O ‰ V-SMOW (Stenni et al., 2010) plotted on a reversed axis. EDC dust (Delmonte et al., 2005) and δ^{18}O (Stenni et al., 2010) data are plotted using the new age scale by Lemieux-Dudon et al. (2010).